

Effect of Random Pinning Sites on Behavior in Josephson-Junction Arrays

Ying-Hong Li and S. Teitel

Department of Physics and Astronomy, University of Rochester, Rochester, New York 14627

(Received 4 June 1991)

We study the effects of dilute random pins on vortex ordering and flow within a bond-diluted Josephson-junction array in a transverse magnetic field. We find evidence suggesting that the disorder drives $T_c \rightarrow 0$; nevertheless, the flux-flow resistivity in a dc current is reduced compared to a pure array.

PACS numbers: 74.60.Ge, 64.60.-i, 74.50.+r, 85.25.Dq

The effect of random pinning centers on vortex ordering and flux-flow resistance in type-II superconductors is an old problem [1] that has received considerable renewed interest in the context of high- T_c superconductors [2], where fluctuations are enhanced. In this Letter, we consider this question in terms of a very simple idealized system, the two-dimensional Josephson-junction array in a transverse magnetic field [3]. We consider a uniform periodic array and compare it with an array in which a controlled amount of dilute randomness has been added. The simplicity of our microscopic model enables us to explore in detail both thermodynamic and steady-state behavior in an applied dc current. Similar models have been studied previously in the context of glassy behavior in granular superconductors [4]. In our model we find evidence suggesting that even a small amount of disorder drives $T_c \rightarrow 0$; there is no true phase-coherent superconducting state. Nevertheless, we find that for the range of temperature and applied current studied, the flux-flow resistivity of the random case is less than the pure case, due to the effects of the pinning centers introduced by the randomness.

The Hamiltonian we consider is defined on a two-dimensional square lattice, and given by

$$\mathcal{H} = - \sum_{\langle ij \rangle} J_{ij} \cos(\theta_i - \theta_j - A_{ij}), \quad (1)$$

where θ_i is the phase of the superconducting wave function at site i , $A_{ij} \equiv (2e/\hbar c) \int_i^j \mathbf{A} \cdot d\mathbf{l}$ is the integral of the vector potential from site i to site j , and the sum is over nearest-neighbor sites. We use a uniform transverse magnetic induction $\mathbf{B} = \nabla \times \mathbf{A}$, for which the sum of A_{ij} around any unit cell equals $2\pi f$, where $f = Ba^2/\Phi_0$ gives the average density-of-field-induced vortices (a is the lattice constant, Φ_0 is the flux quantum). We consider two cases: (i) the *pure* case, where all $J_{ij} = J_0$ a constant, giving a uniform periodic array; (ii) the *random*, or bond-diluted, case, where all $J_{ij} = J_0$ a constant, except for a small fraction p of randomly selected bonds where we set $J_{ij} = 0$. Each missing bond corresponds to a vortex pinning site; the reduced vortex core energy, associated with twisting the phases θ_i by 2π around a unit cell containing a missing bond, results in an effective attraction of the vortices to these sites [5]. Henceforth, energies will be cited in units of J_0 , and lengths in units of a .

We first consider the equilibrium behavior of these two cases, as explored by standard Metropolis Monte Carlo simulations. Our results are for square $L \times L$ lattices with periodic boundary conditions, and a flux density $f = \frac{1}{5}$. The ground-state vortex configuration for the pure case is shown as the inset in Fig. 1. 20000 passes have been used to compute averages, with 5000 initial passes discarded for equilibration. In Fig. 1 we present our results for specific-heat density C , for $L = 20$, as computed from the usual energy fluctuation relation. The pure case shows a clear peak, indicating a transition temperature $T_c \approx 0.18$. On comparison of heating versus cooling, we find hysteresis in the energy density, indicating that the transition in the pure case is first order [6]. In contrast, C for the bond-diluted case appears perfectly smooth, suggesting no finite T_c . Our calculation is for dilution $p = 4\%$, and we have averaged over 32 different realizations of the random bond configuration.

As a better test for phase coherence (and hence superconductivity) consider a "twisted" boundary condition $\theta(x=L, y) - \theta(x=0, y) = \Delta$. For $T < T_c$, the phase coherence across the system results in a total free energy $F(\Delta)$ dependent on the twist, with a total supercurrent flowing $I_s = (2e/\hbar) \langle J_s \rangle_\Delta$, where

$$\begin{aligned} \langle J_s \rangle_\Delta &\equiv \frac{\partial F(\Delta)}{\partial \Delta} \\ &= \frac{1}{L} \left\langle \sum_i J_{i, i+\hat{x}} \sin(\theta_i - \theta_{i+\hat{x}} - A_{i, i+\hat{x}}) \right\rangle_\Delta. \end{aligned} \quad (2)$$

Here $\langle \dots \rangle_\Delta$ denotes a thermal average with a twisted

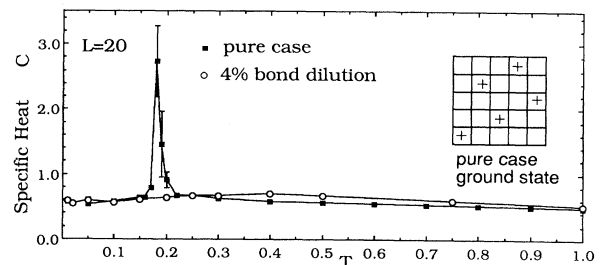


FIG. 1. Specific heat C of the pure and 4% bond-diluted arrays. Inset: A unit cell of the pure-case ground state. $+$ denotes the location of a vortex.

boundary condition given by Δ . $F(\Delta)$ has a periodicity of 2π , and for the pure case its minimum is at $\Delta=0$. For a d -dimensional lattice of length L along the twist, and width W in the transverse directions, the helicity modulus, or "twist stiffness," is defined as [7]

$$Y = \lim_{\Delta \rightarrow 0} \langle J_s \rangle_{\Delta} L / W^{d-1} \Delta = \lim_{\Delta \rightarrow 0} \langle J_s \rangle_{\Delta} / \Delta$$

for $d=2$, $L=W$. For the random case, however, $F(\Delta)$ has its minimum at some Δ_{\min} ($\neq 0$, in general) which varies randomly from sample to sample. For fixed Δ_0 , $\langle J_s \rangle_{\Delta_0}$ may thus have different signs in different samples, and will vanish when averaged over different random bond configurations. Our previous definition of Y must be modified. In this case, an effective twist stiffness may be defined by [8]

$$\bar{Y} \equiv (\overline{\langle J_s \rangle_{\Delta_0}^2})^{1/2}, \tag{3}$$

where the bar denotes the average over different random bond configurations. As Δ_{\min} varies randomly for different samples, our definition of \bar{Y} should be independent of the particular Δ_0 at which it is evaluated [9]. In both the pure and random cases, we should have $Y, \bar{Y} = 0$ for $T > T_c$.

In Fig. 2(a) we plot $Y(T)$ for the pure case, and $\bar{Y}(T)$ for the $p=4\%$ bond-diluted case (averaged over 32 random bond configurations), for several lattice lengths L . In the pure case we see Y independent of L at low T , with $Y \rightarrow 0$ at $T_c \approx 0.18$, the same temperature as the peak in C . In the random case, however, we see that for all temperatures, \bar{Y} decreases as L increases. In Fig. 2(b) we plot $\ln \bar{Y}$ vs $\ln L$ at our lowest temperature $T=0.01$. We see a clear decreasing trend suggesting $\bar{Y} \rightarrow 0$ as $L \rightarrow \infty$, and, hence, no true phase-coherent superconducting state at finite T . This behavior is consistent with recent theoretical arguments concerning the 2D vortex glass [2(a), 2(b)], as well as results for the gauge glass model of a strongly disordered 2D superconductor [10]. Unfortunately, our sizes L are too small for us to extract ex-

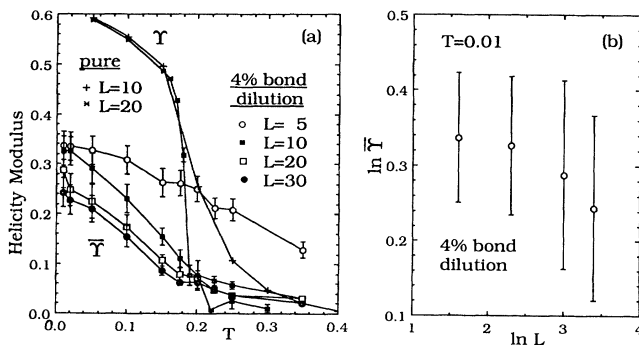


FIG. 2. (a) Helicity modulus Y of the pure and \bar{Y} of the 4% bond-diluted arrays, for various lattice sizes L . (b) $\ln \bar{Y}$ at $T=0.01$ vs $\ln L$. The decreasing \bar{Y} with increasing L suggests $T_c \rightarrow 0$ for the random case.

ponents for the $T_c=0$ critical point, as has been done in this latter model.

We next consider the spatial correlation of the vortices by computing the vortex structure function $S(\mathbf{q}) = \langle n_{\mathbf{q}} n_{-\mathbf{q}} \rangle$, where $n_{\mathbf{q}}$ is the Fourier transform of the vortex density. Using \mathbf{q} along the (2,1) direction (which gives the periodicity of the pure-case ground state), we estimate the spatial correlation length ξ from the half width at half height, Δq , of the peaks of $S(\mathbf{q})$, $\xi \equiv \pi / \Delta q$. These are plotted versus T in Fig. 3(a). For the pure case (we used $L=30$) we find $\xi(T_c^+) \approx 12$ is finite, as expected for a first-order transition [below T_c , $S(\mathbf{q})$ has sharp Bragg peaks]. For the bond-diluted case (we used $L=20$, $p=5\%$, averaged over 32 random bond configurations) $\xi(T=0) \approx 7.5$ is finite, indicating that the ground-state vortex lattice is disordered. Since there are two bonds per site, a 5% bond dilution gives a 10% pin density with an average separation between pins of $a_p = \sqrt{10}$. We find $\xi(T=0) \approx 7.5 > a_p > a_r = \sqrt{5}$, the average separation between vortices at $T=0$. This is in agreement with the theory of weak collective pinning by Larkin and Ovchinnikov [1(a)]. In Fig. 3(b) we plot the average vortex density n_r vs T . No difference is seen between the pure and bond-diluted cases. At low T , $n_r = f = \frac{1}{5}$, the magnetic-field-induced density. At higher $T \sim 1$, n_r increases due to the thermal excitation of additional (+1, -1) vortex pairs.

Now we turn to the dynamic response of the two cases. Using a resistively shunted junction model for the dynamics, we integrate the classical stochastic Langevin equations of motion, as has been described elsewhere [11]. For a uniform current density i injected in one edge and extracted from the other, with periodic boundary conditions in the transverse direction, we compute the average supercurrent density $i_s = I_s / L$ [we use Eq. (2) with $\Delta=0$], which determines the voltage drop per unit length, $V = R_n(i - i_s)$. R_n is the normal shunt resistance across each junction, which we take as a constant parameter.

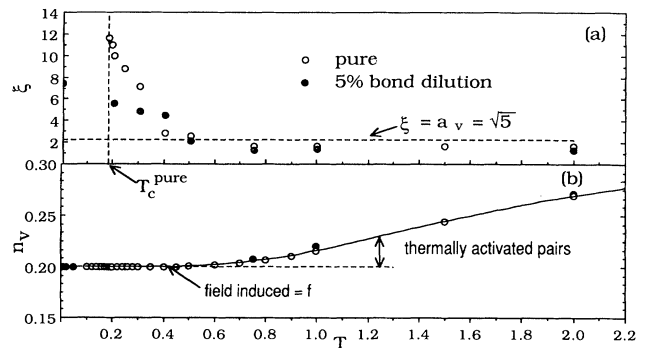


FIG. 3. (a) Vortex spatial correlation length $\xi(T)$ of the pure and 5% bond-diluted arrays, as determined from the width of peaks in the structure function. At high T , $\xi \approx a_r$ is the average spacing between vortices. (b) Vortex density n_r for the pure and random arrays. At low T , $n_r = f = \frac{1}{5}$.

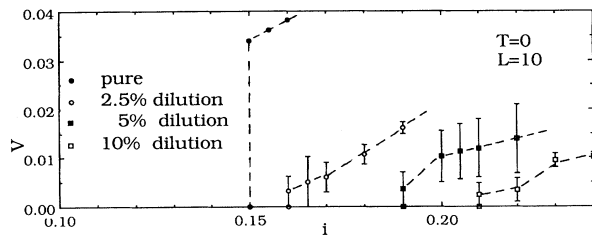


FIG. 4. Voltage per unit length V vs applied current density i at $T=0$ for the pure and $p=2.5\%$, 5% , and 10% bond-diluted arrays. Critical current i_c increases with dilution p .

We integrate typically for 20–40000 time steps of $\Delta t = 0.05(2eR_n i_0/\hbar)$, with an initial 5–10000 steps discarded for equilibration. Henceforth, we measure currents in units of $i_0 = (2e/\hbar)J_0$ (the single junction critical current), voltage in units of $R_n i_0$, and resistivity in units of R_n . In Fig. 4 we show the i - V characteristics computed at $T=0$, on an $L=10$ lattice. The bond-diluted curves are averaged over six realizations of the random bonds, for $p=2.5\%$, 5% , and 10% dilutions. We see that the critical current i_c , at which a nonzero V first appears, increases with increasing p . Our result for the random case, that $i_c(T=0) \neq 0$, while $\bar{Y} \rightarrow 0$ as $T \rightarrow 0$, reflects the irreversibility of the limits $T \rightarrow 0$ and twisting up Δ . Applying a twist Δ and then cooling down temperature T , the system will fall into the minimum-energy configuration $\{\theta_i^0(\Delta)\}$ which carries zero supercurrent (hence, $\bar{Y}=0$). However, once in this energy minimum at $T=0$, increasing the twist to $\Delta + \delta$ can give a finite supercurrent as there is a finite energy barrier between the configurations $\{\theta_i^0(\Delta)\}$ and $\{\theta_i^0(\Delta + \delta)\}$. i_c is a measure of these energy barriers [12].

It is interesting to compare the results above with those of the related problem of tight-binding electrons in a magnetic field [13]. Here the Hamiltonian is $\mathcal{H}_e \psi_i = -\sum_j J_{i,j} e^{iA_{i,j}} \psi_j$, where j are the nearest neighbors of i . For the periodic array, one has a band structure of extended Bloch-like eigenstates. This electron band problem is related to our superconducting problem, by noting that the electron wave function at the band minimum is equal to the superconducting wave function into which the system condenses at T_c , in a linearized Landau-Ginzburg (LG) approximation [14] to our Hamiltonian (1). The electron states about this band minimum correspond to the superconducting states of (1), which one gets by applying finite twists Δ . This problem for a site-diluted lattice has been studied by Soukoulis, Grest, and Li [15]. They show that even a small dilution destroys the commensurate ground-state structures at simple fractions f , and that the states about the band minimum are all *localized*; or correspondingly, the superconducting states in applied twists Δ carry no supercurrent. Assuming the ordered state retains its localized character as one cools down below T_c , we would have $\bar{Y}=0$ in the ordered

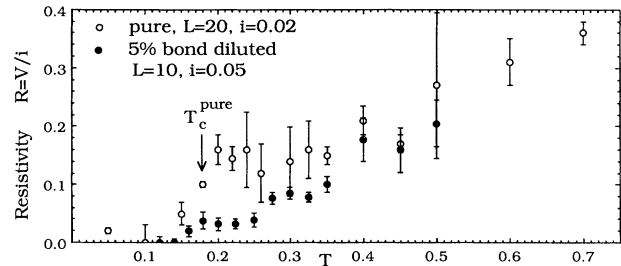


FIG. 5. Flux-flow resistivity $R \equiv V/i$ for the pure and 5% bond-diluted arrays. The pure case shows a sharp drop at $T_c \approx 0.18$ (finite R below T_c is due to nonlinear resistivity). The random case has smaller R due to the effects of pinning.

phase of this linearized LG model.

Finally, we consider the flux-flow resistivity at finite T , defined experimentally [16] as $R \equiv V/i$. Our results are shown in Fig. 5. For the pure case on an $L=20$ lattice with current density $i=0.02 \approx i_c(T=0)/7$, we see the low-temperature plateau in R at $T_c \approx 0.18$, which is characteristic of the first-order, vortex-lattice melting transition [6]. For comparison we show the resistivity R for the random case with $p=5\%$, for $L=10$ and $i=0.05$, averaged over ten random bond configurations [17]. Despite our results suggesting that in the random case $T_c \rightarrow 0$, we see that the flux-flow resistivity is *reduced* from that of the pure case. From Fig. 3(b) we see that the density of vortices from thermally activated vortex pairs is negligible over the temperature range shown for R in Fig. 5. The increase of R with T is therefore due to changing correlations among the field-induced vortices with density f . Comparing Figs. 5 and 3(a) we see that R for the two cases becomes approximately equal when the spatial correlation length $\xi \sim a_c$ at $T \sim 0.5$. At this temperature, vortices move independently of each other. A single pin will trap only one vortex and, hence, a dilute number of pins will have little net effect. At lower T , however, ξ increases, and the vortices move in correlated clusters. Now a single pin can effectively trap a cluster with $\xi^2 f$ vortices. The increased energy barrier for a vortex to move away from a pin reduces the mobility of these vortex clusters and decreases the flux-flow resistivity as compared to the pure case.

We wish to thank Professor Y. Shapir for helpful conversations. We thank Dr. M. P. A. Fisher for pointing out to us Ref. [8], and correcting an error in our original definition of \bar{Y} . This work has been supported by the U.S. Department of Energy under Grant No. DE-FG02-89ER14017. Computations were carried out as part of DOE sponsored research at the Florida State University Supercomputer Center.

[1] (a) A. I. Larkin and Yu. N. Ovchinnikov, J. Low Temp.

- Phys. **34**, 409 (1979); (b) P. W. Anderson and Y. B. Kim, Rev. Mod. Phys. **36**, 39 (1964).
- [2] (a) M. P. A. Fisher, Phys. Rev. Lett. **62**, 1415 (1989); (b) D. S. Fisher, M. P. A. Fisher, and D. A. Huse, Phys. Rev. B **43**, 130 (1991); (c) R. S. Markiewicz, Physica (Amsterdam) **171C**, 479 (1990); (d) D. R. Nelson and P. Le Doussal, Phys. Rev. B **42**, 10113 (1990).
- [3] S. Teitel and C. Jayaprakash, Phys. Rev. B **27**, 598 (1983); Phys. Rev. Lett. **51**, 1999 (1983).
- [4] W. Y. Shih, C. Ebner, and D. Stroud, Phys. Rev. B **30**, 134 (1984); C. Ebner and D. Stroud, Phys. Rev. B **31**, 165 (1985); X. C. Zheng, D. Stroud, and J. S. Chung, Phys. Rev. B **43**, 3042 (1991); S. John and T. C. Lubensky, Phys. Rev. Lett. **55**, 1014 (1985); Phys. Rev. B **34**, 4815 (1986).
- [5] M. B. Cohn, M. S. Rzchowski, S. P. Benz, and C. J. Lobb, Phys. Rev. B **43**, 12823 (1991).
- [6] Similar results were seen for the $f = \frac{2}{3}$ case in Y.-H. Li and S. Teitel, Phys. Rev. Lett. **65**, 2595 (1990).
- [7] M. E. Fisher, M. N. Barber, and D. Jasnow, Phys. Rev. A **8**, 1111 (1973).
- [8] For general dimension d one has $L^{d-2}\bar{Y} = (\overline{J_s^2/\Delta_0^2})^{1/2} \sim L^\theta$, where $\theta=0$ and T_c , and $0 \leq \theta \leq d-2$ for $T < T_c$. This method has been applied to behavior in the 3D "gauge glass" model by J. D. Reger, T. A. Tokuyasu, A. P. Young, and M. P. A. Fisher, Phys. Rev. B **44**, 7147 (1991).
- [9] The results for \bar{Y} in Fig. 2 are computed for the arbitrarily chosen value $\Delta_0 = \pi/6$. We have checked for possible dependence on Δ_0 by also computing \bar{Y} with $\Delta_0 = \pi/2$, on the $L=10$ lattice. For the two values of Δ_0 , we find $\bar{Y}(T)$ remains the same, within our statistical error.
- [10] M. P. A. Fisher, T. A. Tokuyasu, and A. P. Young, Phys. Rev. Lett. **66**, 2931 (1991); M. J. P. Gingras, Ecole Normale Supérieure report, 1991 (to be published).
- [11] K. K. Mon and S. Teitel, Phys. Rev. Lett. **62**, 673 (1989); J. S. Chung, K. H. Lee, and D. Stroud, Phys. Rev. B **40**, 6570 (1989); F. Faló, A. R. Bishop, and P. S. Lomdahl, Phys. Rev. B **41**, 10983 (1990); S. R. Shenoy, J. Phys. C **18**, 5163 (1985).
- [12] As one averages over more realizations of the random bonds, the i - V curves in Fig. 4 may develop low-current tails at small i , perhaps extending to $i=0$ as $L \rightarrow \infty$, arising from particular configurations in which the missing bonds form long connected paths; see W. Xia and P. L. Leath, Phys. Rev. Lett. **63**, 1428 (1989); P. L. Leath and W. Xia, Rutgers University report, 1991 (to be published). The values of i_c seen in Fig. 4 thus give the heights of typical barriers to vortex motion, rather than the true critical current in the thermodynamic limit.
- [13] D. R. Hofstadter, Phys. Rev. B **14**, 2239 (1976).
- [14] S. Alexander, Phys. Rev. B **27**, 1541 (1983); S. Teitel and C. Jayaprakash, J. Phys. (Paris), Lett. **46**, L33 (1985).
- [15] C. M. Soukoulis, G. S. Grest, and Q. Li, Phys. Rev. B **38**, 12000 (1988).
- [16] Since our simulations are for finite $i > 0$, $R \equiv V/i$ will differ from the true linear resistivity below and slightly above T_c , where nonlinear effects are important. This explains the finite resistive tail seen below T_c in Fig. 5. See also Ref. [6].
- [17] The smaller L and larger i for the random case was necessary in order to reduce the statistical fluctuations with R larger than the pure case due to the additional averaging over random configurations. If we consider the pure case at these same L and i , we find virtually the same values of R as those shown in Fig. 4, except that the plateau at T_c becomes smoothed out, and there is a broader tail below T_c due to the increased nonlinear resistivity.